A plasma cell differentiation quality control ablates B cell clones with biallelic Ig rearrangements and truncated Ig production

Nivine Srour,[1] Guillaume Chemin,[1]* Aurélien Tinguely,[1]* Mohamad Omar Ashi,[1] Zéliha Oruc,[1] Sophie Péron,[1] Christophe Sirac,[1] Michel Cogné,[1,2]** and Laurent Delpy[1]**

[1]Centre National de la Recherche Scientifique UMR 7276 and [2]Institut Universitaire de France, Université de Limoges, 87000 Limoges, France

Aberrantly rearranged immunoglobulin (Ig) alleles are frequent. They are usually considered sterile and innocuous as a result of nonsense-mediated mRNA decay. However, alternative splicing can yield internally deleted proteins from such nonproductively V(D)J-rearranged loci. We show that nonsense codons from variable (V) Igκ exons promote exon-skipping and synthesis of V domain–less κ light chains (ΔV-κLCs). Unexpectedly, such ΔV-κLCs inhibit plasma cell (PC) differentiation. Accordingly, in wild-type mice, rearrangements encoding ΔV-κLCs are rare in PCs, but frequent in B cells. Likewise, enforcing expression of ΔV-κLCs impaired PC differentiation and antibody responses without disturbing germinal center reactions. In addition, PCs expressing ΔV-κLCs synthesize low levels of Ig and are mostly found among short-lived plasmablasts. ΔV-κLCs have intrinsic toxic effects in PCs unrelated to Ig assembly, but mediated by ER stress–associated apoptosis, making PCs producing ΔV-κLCs highly sensitive to proteasome inhibitors. Altogether, these findings demonstrate a quality control checkpoint blunting terminal PC differentiation by eliminating those cells expressing nonfunctionally rearranged Igκ alleles. This truncated Ig exclusion (TIE) checkpoint ablates PC clones with ΔV-κLCs production and exacerbated ER stress response. The TIE checkpoint thus mediates selection of long-lived PCs with limited ER stress supporting high Ig secretion, but with a cost in terms of antigen-independent narrowing of the repertoire.

During early B cell maturation, Ig loci undergo programmed DNA rearrangements of germline V (variable), D (diversity), and J (joining) gene segments. This error-prone program generates random V(D)J junctions and a diversified primary antibody repertoire (Jung et al., 2006). Functional Ig heavy (H) and light (L) chains are controlled at the stages of pre–B cell receptor (preBCR) and BCR expression, respectively (Melchers et al., 2000). These early checkpoints ensure expansion of B cells expressing functional Ig chains, while limiting the development of autoreactive clones (Rajewsky, 1996). Once positively selected, immature B cells transit to the periphery and join the mature B cell pool. Upon antigen (Ag) stimulation, germinal center (GC) B cells diversify their receptors through activation-induced cytidine deaminase (AID)–dependent somatic hypermutation (SHM) and class-switch recombination (CSR; Manis et al., 2002; Pavri and Nussenzweig, 2011; Andrews et al., 2013). Self-reactive clones are also tightly controlled in mature and GC B cells, and BCR-signal strength regulates these late tolerance checkpoints, eventually leading to anergy or elimination of B cells (Allen et al., 2007; Victora and Nussenzweig, 2012). Our group has recently demonstrated that a recombination by IgH locus suicide recombination (LSR) participates actively in the late elimination of GC B cells (Péron et al., 2012). Cells that survive negative selection further differentiate into either memory B cells or plasma cells (PCs) secreting high-affinity antibodies. PCs are antibody-producing factories in which a massive expansion of the endoplasmic reticulum (ER), together with elevated production of chaperone proteins such as GRP78/BiP (glucose-regulated protein 78 kD/binding immunoglobulin protein), ensures proper folding and secretion of large amounts of Ig (Gass et al., 2002; Ron and Walter, 2007; Todd et al., 2009). Major transcriptional changes accompany PC differentiation, including a boost of Ig gene expression and modification of their splicing pattern, from membrane-type toward secretory-type Ig mRNAs (Santos et al., 2011).

Random nucleotide additions or deletions at V(D)J junctions inherently yield frameshifts and premature stop codons in two thirds of cases (Jung et al., 2006). When a nonproductive

*G. Chemin and A. Tinguely contributed equally to this paper.

**M. Cogné and L. Delpy contributed equally to this paper.

Correspondence to Laurent Delpy: laurent.delpy@unilim.fr; or Michel Cogné: michel.cogne@unilim.fr

Abbreviations used: Ag, antigen; AID, activation-induced cytidine deaminase; AS, alternative splicing; CHOP, C/EBP homologous protein; CSR, class-switch recombination; ΔV-κLC, variable domain-less Igκ light chain; ER, endoplasmic reticulum; GC, germinal center; κLC, Igκ light chain; LSR, locus suicide recombination; NAS, nonsense-associated altered splicing; NMD, nonsense-mediated mRNA decay; PC, plasma cell; PI, proteasome inhibitor; PTC, premature termination codon; SHM, somatic hypermutation; TIE, truncated Ig exclusion.

The Rockefeller University Press $30.00
J. Exp. Med. 2016 Vol. 213 No. 1 109–122
www.jem.org/cgi/doi/10.1084/jem.20131511

V(D)J junction first affects one Ig allele, the second allele can still productively rearrange and support B cell maturation. Such biallelic V(D)J rearrangements, including a nonproductive allele, are retrieved in ∼40–50% of B lymphocytes (Mostoslavsky et al., 2004; Daly et al., 2007). It is now well accepted that nonproductive Ig alleles are actively transcribed during B cell development (Singh et al., 2003; Delpy et al., 2004a,b; Daly et al., 2007; Eberle et al., 2009; Tinguely et al., 2012; Holwerda et al., 2013). The nonsense-mediated mRNA decay (NMD) pathway ensures efficient degradation of the resulting Ig mRNAs harboring premature termination codons (PTCs), and hence limits the production of truncated Ig with C-terminal deletions (Li and Wilkinson, 1998). NMD likely protects lymphoid cells from adverse effects of aberrant Ig transcripts. Indeed, disruption of lymphocyte development was observed upon either expression of an UPF1 (up-frameshift protein 1) dominant-negative isoform (Frischmeyer-Guerrerio et al., 2011) or conditional deletion of *Upf2* (Weischenfeldt et al., 2008), two major NMD actors. In addition, Lutz et al. (2011) observed that the persistence of nonsense μH mRNAs escaping effective NMD degradation impairs pro–B cell differentiation.

Abnormal RNA splicing is elicited upon recognition of nonsense mutations by the RNA surveillance machinery, leading to the accumulation of unspliced PTC-containing premRNAs or to the appearance of alternatively spliced mRNAs (Valentine, 1998; Maquat, 2002; Lejeune and Maquat, 2005). Several studies, including ours, have documented that in addition to NMD, nonproductive Ig transcripts are surveyed by the cooperative action of splicing inhibition and nonsense-associated altered splicing (NAS; Aoufouchi et al., 1996; Mühlemann et al., 2001; Bühler and Mühlemann, 2005; Chemin et al., 2010; Tinguely et al., 2012). Unlike NMD, which prevents the translation of prematurely terminated Ig polypeptides, nothing is known about the consequence of NAS and exon skipping with regard to the production of mRNAs and proteins with internal deletions. Production of shortened Ig chains and exon skipping occurs in pathologies such as heavy chain diseases and monoclonal Ig deposition diseases (Cogné et al., 1988, 1992). In contrast, truncated Ig chains have never been documented in normal B cells, and whether aberrant Ig transcripts from excluded alleles end up with aberrant peptides is an open question. To address this issue during B cell development and PC differentiation, we analyzed the splicing pattern of Igκ transcripts. These simplest RNA molecules include only three exons: leader (L), variable (V), and constant (C). We found that the presence of nonsense codons within the V exon modified the splicing of Igκ transcripts and strongly enhanced exon skipping. Interestingly, the production of V domain-less κ light chains (ΔV-κLCs) exacerbated the ER stress response and severely impaired PC differentiation. Thus, the transcription of nonproductively rearranged Ig alleles can be detrimental at some differentiation stages. Collectively, these findings reveal a late quality control process dedicated to truncated Ig exclusion (TIE). This TIE checkpoint blunts ∼20–25% of terminally differentiated PCs by eliminating in an Ag-independent manner half of those 40–50% cells with biallelic rearrangements of Igκ alleles.

RESULTS

Nonsense codons located within V regions enhance exon skipping of Igκ transcripts

We previously showed in normal B lineage cells that upon skipping of some noncoding V exons, so called excluded alleles often yield shortened κ mRNAs which would translate into ΔV-κLCs (Chemin et al., 2010). Observing such shortened mRNAs is surprising because the production of truncated Ig is usually considered a specific feature of some lymphoproliferative diseases (Cogné et al., 1992). To extend this study, we further analyzed the conditions of exon skipping, checked whether shortened Igκ transcripts were translated into ΔV-κLCs, and addressed whether the latter affects B cell differentiation. Out-of-frame Vκ-to-Jκ rearrangements result in nonsense codons affecting either the 3′-end of the V exon (V^{PTC}) or the C exon (C^{PTC}; Delpy et al., 2004a; Fig. 1 A). We compared ΔV-κLC mRNA levels in cell lines transfected with constructs mimicking nonproductive VκJκ5 rearrangements from both the V^{PTC} and the C^{PTC} class (Fig. 1, B and C). This revealed high ΔV-κLC mRNAs in V^{PTC}-expressing cells, whereas such transcripts were barely detectable in C^{PTC}-expressing cells and absent in cell lines expressing productive Igκ genes (Fig. 1 D). ΔV-κLC mRNA levels were quantified using capillary electrophoresis after normalization to the amount of productive κLC mRNAs, as previously described (Chemin et al., 2010). Compared with C^{PTC}-expressing cells, ΔV-κLC mRNAs were ∼3.5- and 6.7-fold higher in V^{PTC}-expressing B (A20) and PC (S194) lines, respectively (Fig. 1 E). Hence, skipping of the V exon occurs mostly when this exon itself carries the PTC, and with an efficiency approximately two times higher in PCs than in B cells.

Exacerbated ER stress response in PCs expressing ΔV-κLCs

Next, we checked whether ΔV-κLC mRNAs were indeed translated into of V domain-less truncated Ig, thus expected to mostly show up in V^{PTC}-expressing PCs. Consistent with data in Fig. 1, complete κLCs (∼25 kD) and truncated ΔV-κLCs (∼12 kD) were detected in cells transfected with productive and V^{PTC} constructs, respectively (Fig. 2 A). In contrast, no ΔV-κLCs (or a background level similar to nonsecretory Sp2/0 cells) was observed in untreated C^{PTC}-expressing cells (Fig. 2 A). We further explored whether ΔV-κLCs were routed toward proteasomal degradation. In V^{PTC}-expressing cells, treatment with MG132 induced an approximately two- to four-fold increase of ΔV-κLCs in cell pellets and culture supernatants, respectively (Fig. 2, A and B). In contrast in C^{PTC}-expressing cells, very low amounts of ΔV-κLCs were found in cell pellets, and only upon treatment with MG132 (Fig. 2 A). For controls, no major changes were observed for complete κLCs (Fig. 2, A and B).

The survival of PCs depends on their ability to alleviate the ER stress response associated with massive Ig synthesis

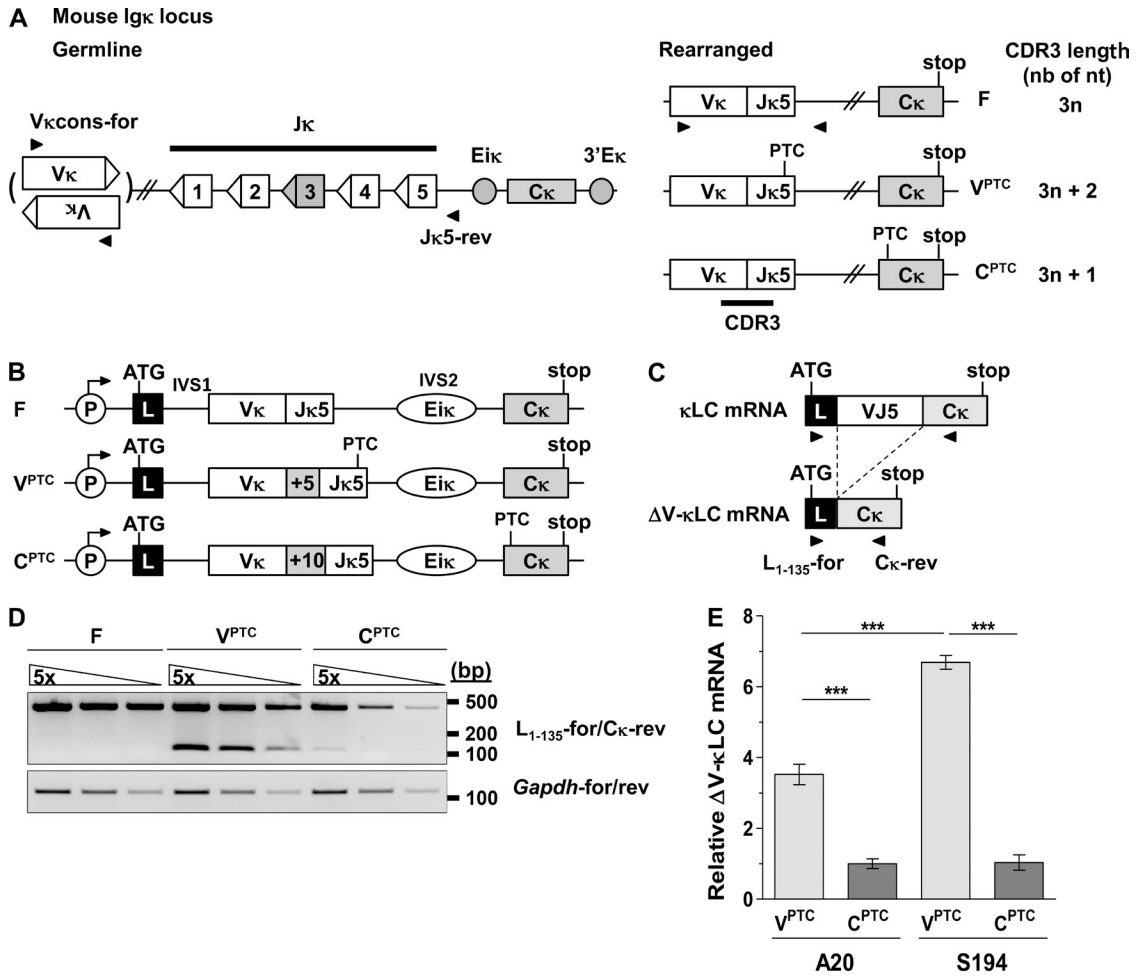

Figure 1. **Alternative splicing of nonproductive Igκ transcripts in B cell and plasma cell lines.** (A, left) Mouse Igκ locus showing Vκ segments (in normal and inverse orientations), the four functional Jκ segments, the intronic κ enhancer (Eiκ), and the constant Cκ exon. (right) In-frame (F) and out-of-frame (V^{PTC} and C^{PTC}) VκJκ5 junctions are depicted, and the position of normal stop codons (stop) and PTCs are shown. Primers used are indicated (black arrows). (B) Representation of in-frame (F), V^{PTC}, and C^{PTC} mini-gene constructs. Out-of-frame junctions were created by inserting 5 nt (V^{PTC}) or 10 nt (C^{PTC}) at VκJκ5 junctions. (C) RT-PCR was performed using L_{1-135}-for/Cκ-rev primers to identify full-length (κLC) and alternatively spliced (ΔV-κLC) mRNAs simultaneously. (D) Semiquantitative RT-PCR analysis of S194 cell lines transfected with F, V^{PTC}, and C^{PTC} constructs. (E) A20 (mature B) and S194 (PC) cell lines were cotransfected with F and either V^{PTC} or C^{PTC} constructs (A20-F+V^{PTC}, $n = 9$; A20-F+C^{PTC}, $n = 5$; S194-F+V^{PTC}, $n = 6$; S194-F+C^{PTC}, $n = 5$). Relative ΔV-κLC mRNA levels were quantified using capillary electrophoresis by dividing areas of peaks corresponding to ΔV-κLC mRNAs to those of control functional (F) κLC mRNAs (ΔV-κLC/F ratios) as previously described (Chemin et al., 2010); part of these data (A20-F+V^{PTC}, $n = 4$; S194-F+V^{PTC}, $n = 3$) comes from this previous study. Data are representative of at least three independent experiments ($n = 5$–9). Bars represent mean expression ± SEM. Unpaired two-tailed Student's test was performed to determine significance. ***, $P < 0.001$.

(Cenci et al., 2011). PC survival might thus be impacted by the production of proteins with abnormal structures and folding. To address this issue, we analyzed the apoptotic index of S194 PCs with regard to the abundance of ΔV-κLCs. Interestingly, V^{PTC}-expressing cells exhibit higher apoptosis than nontransfected and C^{PTC}-expressing cells, upon treatment with MG132 (Fig. 2 C). In addition, mRNA levels of *C/EBP homologous protein* (*Chop*), a transcription factor involved in ER-stress induced apoptosis (Obeng et al., 2006), were approximately two-fold higher in V^{PTC}-expressing cells than in nontransfected cells upon treatment with MG132 (Fig. 2 D). As expected, *Chop* expression in C^{PTC}-expressing cells was intermediate, in between nontransfected and V^{PTC}-expressing cells (Fig. 2 D). Therefore, the presence of ΔV-κLCs likely provokes excessive ER-stress that sensitizes plasma cells to CHOP-dependent apoptosis upon proteasome inhibition.

A TIE checkpoint counterselects those PCs expressing V^{PTC}-rearranged Igκ alleles

Differential sensitivity to apoptosis can hardly be followed in vivo due to immediate phagocytosis of apoptotic cells. However, such differences would be expected to result in a bias in

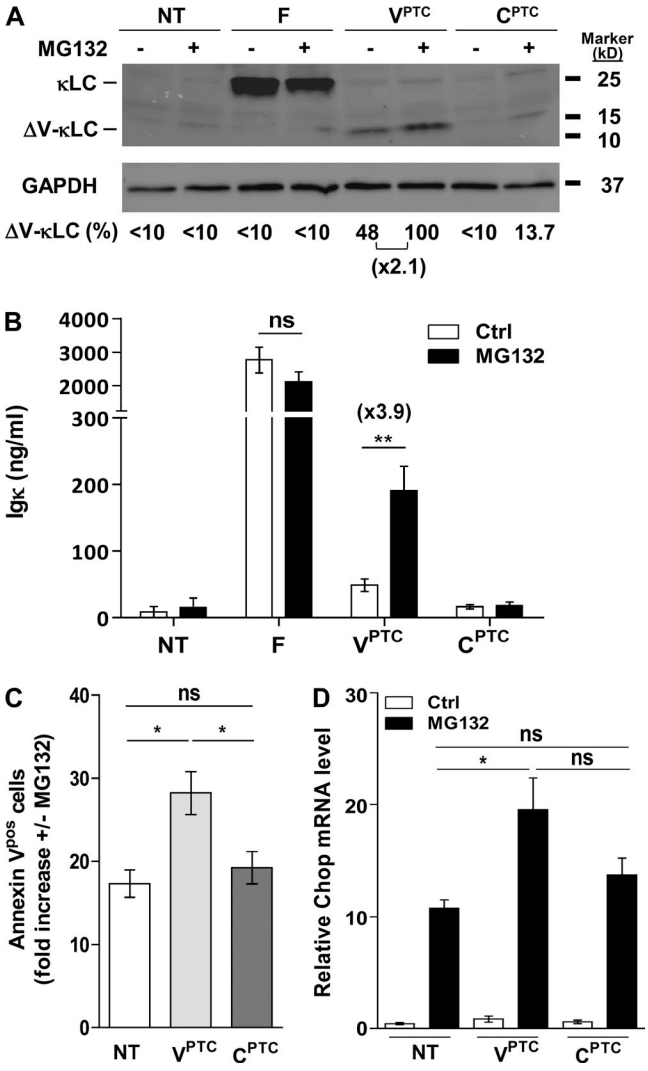

Figure 2. **Production of truncated Ig and exacerbated ER stress response in V^{PTC}–expressing cells lines.** Sp2/0 (hybridoma) clones isolated after transfection with F (n = 5), V^{PTC} (n = 6), or C^{PTC} (n = 5) constructs were treated or not with MG132 (1 µM, 8 h). Complete κLCs (25 kD) and truncated ΔV-κLCs (12 kD) were assessed by Western blot (A) and ELISA (B) on cell pellets and culture supernatants, respectively. (A) A representative experiment from a pool of four clones per group is shown. (B) ELISA assays were performed in all transfected cells using anti-Igκ Abs. (C) Annexin V staining was performed in S194 cells either nontransfected (NT) or transfected with V^{PTC} (n = 9) and C^{PTC} (n = 6) constructs, and treated or not with MG132 (1 µM, 5 h). (D) In those cells, *Chop* mRNA levels were assessed by Q-PCR. Data are representative of two (A and B) or three (C and D) independent experiments (n = 5–9). Bars represent mean expression ± SEM. Unpaired two-tailed Student's test was performed to determine significance. *, P < 0.05; **, P < 0.01.

the selection of terminally differentiated cells, thus providing indirect arguments for a TIE checkpoint. To address this issue, we analyzed the Igκ repertoire at the DNA level in B cells and PCs from WT animals. We determined CDR3 lengths and distinguished in-frame (F or VJ^+) V^{PTC} and C^{PTC} VκJκ junctions (Fig. 1 A). In agreement with previous works (Chen et al., 1993; Ehlich et al., 1993; Novobrantseva et al., 1999; Bertocci et al., 2003; Delpy et al., 2004a), VκJκ5 junctions were readily detectable in precursor B cells that did not express a BCR (pro–B/pre–B cells: $B220^{lo}/IgL^{neg}$). As expected, numerous (~66.6%) out-of-frame junctions were retrieved in the absence of BCR-mediated selection, with an equivalent repartition of V^{PTC} and C^{PTC} subclasses (Table 1). In contrast, the percentage of F junctions was much higher in GC B cells ($B220^{hi}/PNA^{hi}$) having been selected for functional BCR expression, with a reciprocal fall of V^{PTC} and C^{PTC} subclasses (Table 1). Unexpectedly, the frequency of V^{PTC} junctions still more drastically decreased in PCs ($B220^{neg}/CD138^{pos}$; approximately nine-fold lower than GC B cells; $P < 0.01$), whereas that of C^{PTC} junctions was unchanged (Table 1). Next, we addressed whether the disappearance of PCs harboring V^{PTC}-rearranged Igκ alleles prone to exon-skipping correlated with a decrease in ΔV-κLC mRNAs. ΔV-κLC mRNA levels were analyzed by RT-PCR in sorted B cell populations and PCs (Fig. 3 A). Although, a short band corresponding to ΔV-κLC mRNAs was readily detectable in B cell populations, these alternative transcripts were not retrieved in PCs (Fig. 3, B and C). The complete loss of ΔV-κLC mRNAs in PCs was consistent with the drastic disappearance of V^{PTC} junctions in their repertoire. Altogether, the selective elimination of PCs with biallelic Igκ rearrangements in VJ^+/V^{PTC} configuration, likely reflects toxic effects of ΔV-κLCs. This suggests that, independently of B cell functionality and specificity for antigen, a late TIE checkpoint counterselects B lineage cells producing aberrant Ig and prevents their survival as terminally differentiated PCs.

Impaired PC differentiation upon inducible expression of ΔV-κLCs

According to previous observations showing that ~40–50% of B lymphocytes exhibit biallelic V(D)J rearrangements of Ig genes (Mostoslavsky et al., 2004; Daly et al., 2007), approximately half of these B cell clones (~20–25%), i.e., those harboring V^{PTC}-rearranged Igκ alleles, are candidates for an Ag-independent TIE checkpoint, eventually leading to their elimination at the step of PC differentiation. However, the rarity of V^{PTC} junctions in PCs at the DNA level is only an indirect proof that cells go through such a checkpoint. To directly address the impact of ΔV-κLCs on late B cell development and on humoral responses, we created Igκ knock-in mice allowing inducible expression of ΔV-κLCs in B lineage cells (Fig. 4 A). In these mutants, later referred as inducible TIE (iTIE) mice, the replacement of endogenous Jκ segments by a leader exon ($L_{1\text{-}33}$) under the control of a pV_H promoter led to enforced expression of ΔV-κLC mRNAs and proteins. Conditional Cre-mediated expression of ΔV-κLC mRNAs was achieved by inserting a *lox*P-flanked neomycin-resistance (NeoR) cassette that blocks transcription and splicing of the $L_{1\text{-}33}$ exon (Fig. 4 A). In heterozygous (iTIE/+) animals, the WT allele (+) supports normal Igκ expression during B

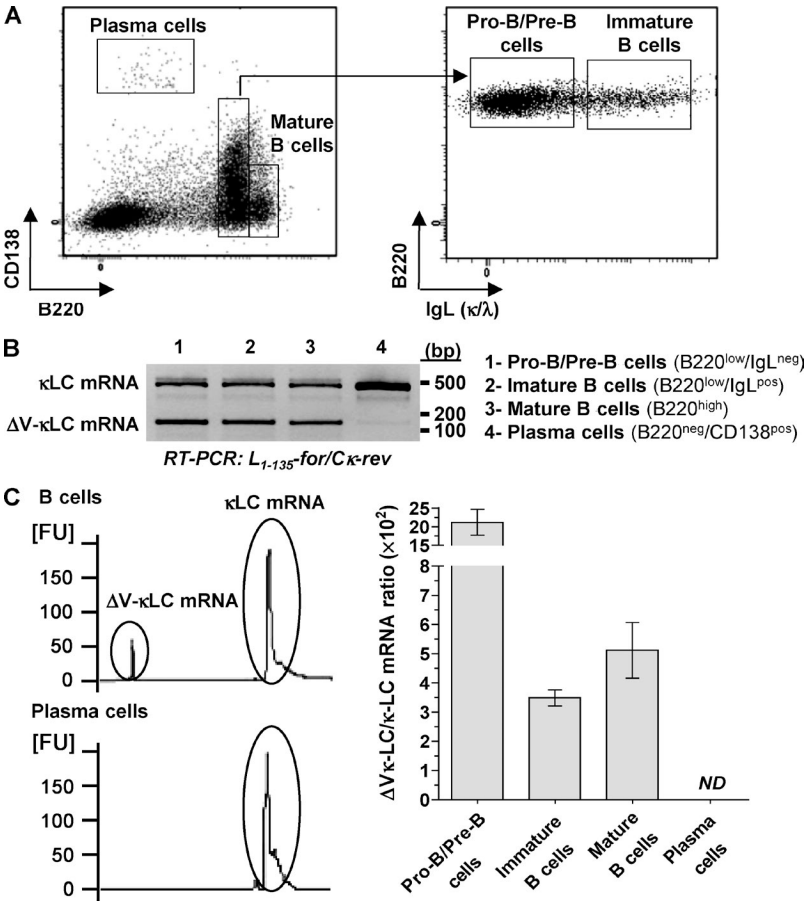

Figure 3. **Exon skipping of Igκ transcripts occurs in normal B cells but not in PCs.** (A) Primary B and plasma cells were isolated from bone marrow and sorted after staining with anti-B220, anti-IgL (κ and λ), and anti-CD138 mAbs. Representative dot plots and gates used for cell sorting are depicted. The purity of sorted populations was always >90%. (B) RT-PCR was performed using $L_{1\text{-}135}$ forward and constant Cκ reverse primers to analyze both full-length κLC and ΔV-κLC mRNA levels in sorted cell populations. One representative experiment is shown. (C) Quantification of amplification products was done using an Agilent Bioanalyzer (left). ΔV-κLC/κLC mRNA ratios were determined for each sorted populations ($n = 3$; right). FU, fluorescence unit. Bars represent mean expression ± SEM. Data are representative of three independent experiments using a pool of two B6 mice per experiment.

cell development, whereas the knock-in (iTIE) allele allows Cre-dependent expression of ΔV-κLCs. After mating iTIE/+ mice with a CMV-Cre–expressing strain, high ΔV-κLC mRNA levels and significant truncated Ig synthesis were observed in Cre-positive (Cre^{pos}) B lineage cells, with no major leakiness in Cre-negative (Cre^{neg}) controls (Fig. 4 B). In agreement with the aforementioned data from transfected cells (Fig. 2), ΔV-κLC amounts increased after treatment with the proteasome inhibitor bortezomib (Bz; Fig. 4 B). Interestingly, these knock-in mice mimic the outcome of the physiological TIE checkpoint, as the production of ΔV-κLCs severely impairs PC differentiation without perturbing B cell development and GC formation (Fig. 4, C and D). In controls, the sole expression of Cre-recombinase affected neither total $B220^{pos}$ and GC B cells nor PCs (unpublished data). Consistent with a global defect in PC differentiation, Cre^{pos} iTIE/+ mice exhibited significantly lower T cell–independent and T cell–dependent antibody responses than Cre^{neg} iTIE/+ controls (Fig. 4, E and F). These findings were further confirmed in competitive experiments mimicking the occurrence of the TIE checkpoint during late B cell differentiation and in only a fraction of terminally differentiated PCs. For that, we analyzed B cell and PC contents after mating iTIE mice with AID-Cre-EYFP mice, allowing conditional Cre-recombinase expression in GC B cells upon treatment with tamoxifen (Dogan et al., 2009). We found significantly lower amounts of

Table 1. **Analysis of productive and nonproductive VκJκ5 junctions in B and plasma cells from WT mice**

Cell type	Total	In-frame	V^{PTC}	C^{PTC}
	n	%	%	%
Pro-B/pre-B cells	51	33.3	31.4	35.3
GC B cells	53	60.4	18.9	20.7
Plasma cells	47	72.3	2.1	25.5

Pro-B/pre-B cells ($B220^{lo}/IgL^{neg}$) and PCs ($B220^{neg}/CD138^{pos}$) were isolated from bone marrow and GC B cells ($B220^{hi}/PNA^{hi}$) from Peyer's patches, and PCRs were performed on genomic DNA using Vκcons-for/Jκ5-rev primers (Fig. 1 A). Productive VκJκ5 junctions were assigned as in-frame and nonproductive junctions as V^{PTC} and C^{PTC}. Data are from two independent cell sorting experiments. *n* = total number of sequences.

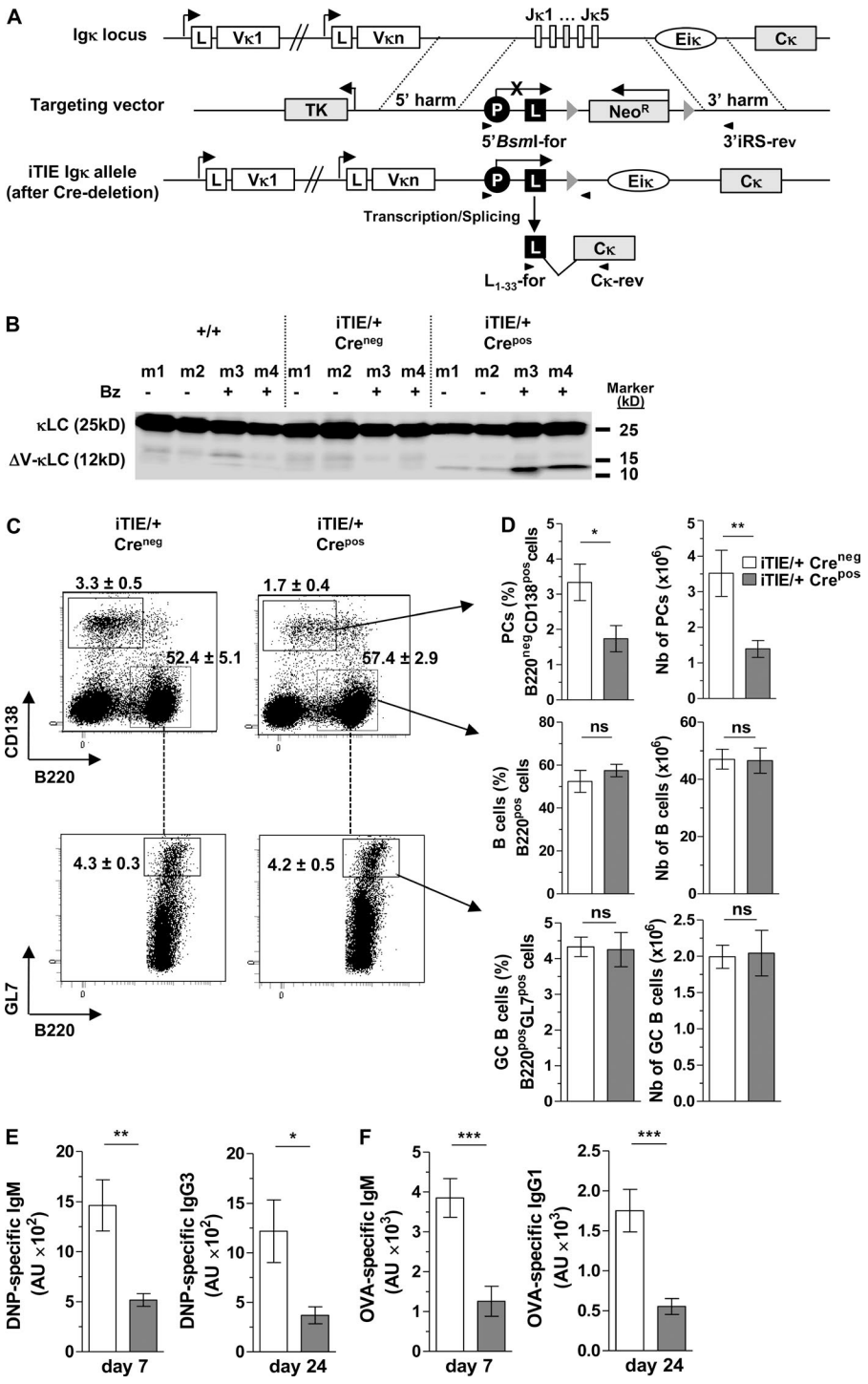

Figure 4. **Altered plasma cell differentiation and antibody responses in model mice reproducing the TIE checkpoint.** (A) Gene targeting strategy. Map of the Igκ locus in germline configuration (top), after Jκ replacement (middle), and Cre-mediated recombination of the *lox*P-flanked *hsv*TK-Neo^R cassette (bottom). (B) Western blot analysis of complete κLCs and truncated ΔV-κLCs performed on spleen cells from WT (+/+) and iTIE/+ mice 6 d after IP injection of SRBCs. At day 4 and 5, mice received additional IP injections of PBS (−) or bortezomib (+Bz). A representative experiment using four mice per genotype is shown. (C) FACS analysis was performed on spleen cells isolated 6 to 7 d after SRBC injection. (D) The percentage (left) and absolute numbers (right) of PCs (B220^{neg}/CD138^{pos}; top), B cells (B220^{pos}; middle), and GC B cells (B220^{pos}/GL7^{pos}; bottom) are shown for Cre^{pos} (gray bars) and Cre^{neg} iTIE/+ (empty bars; n = 16 mice/group). (E and F) Cre^{pos} (gray) and Cre^{neg} (empty) iTIE/+ mice (n = 8/group) were immunized with two IP injections (day 0 and 14) of DNP-Ficoll (E) and OVA (F). Sera were collected at day 7 and 24 and ELISA assays were performed to determine DNP- (E) and OVA- (F) specific IgM (left), IgG3 (E, right), and IgG1 (F, right) titers. Data are from two (B) and at least three (C–F) independent experiments. n = 8–16. Bars represent mean expression ± SEM. Unpaired two-tailed Student's test was performed to determine significance. *, P < 0.05; **, P < 0.01; ***, P < 0.001.

EYFP-positive PCs in AID-Cre-EYFP iTIE/+ mice, compared with AID-Cre-EYFP +/+ littermates (Fig. 5, A and B). In contrast, similar frequency and absolute numbers of EYFP-positive B cells were retrieved in these animals (Fig. 5, C and D). Thus, the PC defect observed in Cre^{pos} iTIE mice confirms that the production of ΔV-κLCs induces deleterious effects in terminally differentiated B lineage cells.

Short lifespan and low levels of Ig secretion in PCs expressing ΔV-κLCs

Next, we sought to elucidate how these truncated Ig control plasma cell maturation using the iTIE mouse model with enforced ΔV-κLC expression. Experiments were performed in homozygous iTIE/iTIE animals that have no functional Igκ alleles and exhibit only Igλ-expressing B lineage cells. Like

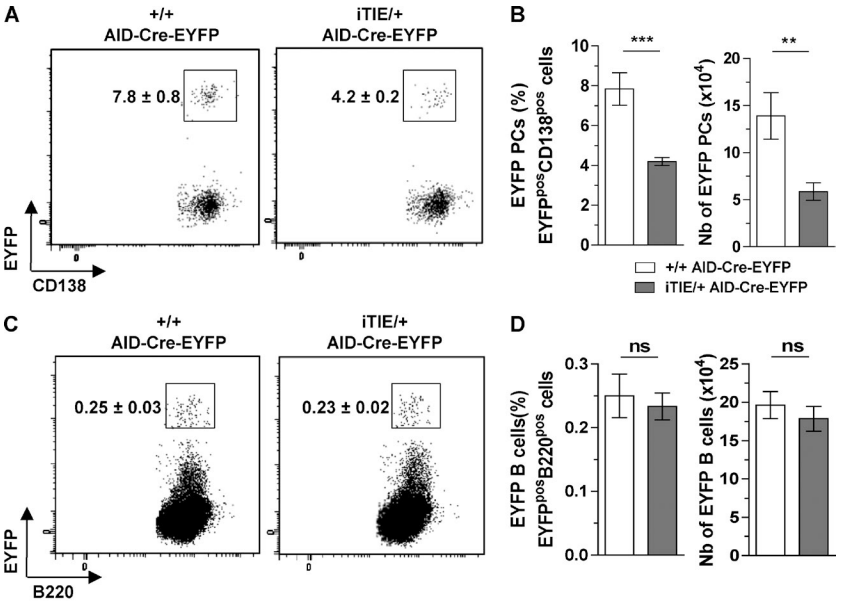

Figure 5. **Altered plasma cell differentiation after inducible production of truncated Ig in germinal center B cells.** FACS analysis was performed on spleen cells after gating on $B220^{neg}/CD138^{pos}$ PCs (A) or $B220^{pos}$ B cells (C), as depicted in Fig. 4 C. The frequency and absolute numbers of $EYFP^{pos}$ PCs (B) and $EYFP^{pos}$ B cells (D) were determined 7 d after IP injections of SRBCs in tamoxifen-treated WT (+/+; $n = 6$) and iTIE/+ ($n = 6$) mice on AID-Cre-EYFP background. Data are from two independent experiments. Bars represent mean expression ± SEM. Unpaired two-tailed Student's test was performed to determine significance. **, $P < 0.01$; ***, $P < 0.001$.

heterozygous mutant mice (Cre^{pos} iTIE/+), but to a higher extent, homozygous animals (Cre^{pos} iTIE/iTIE) exhibited very low amounts of $B220^{neg}CD138^{pos}$ PCs (Fig. 6 A) together with a strong reduction in serum Ig levels (Fig. 6 B), compared with Cre^{neg} controls. ΔV-κLC mRNA amounts were determined by qPCR in B cells and PCs isolated from bone marrow of Cre^{pos} iTIE/iTIE mice. We found that the remaining PCs exhibited approximately five-fold higher ΔV-κLC mRNA levels compared with sorted B cells (Fig. 6 C). To evaluate whether ΔV-κLC production in PCs affected Ig synthesis, we analyzed the expression of Igλ in Cre^{pos} and Cre^{neg} iTIE/iTIE $B220^{neg}CD138^{pos}$ PCs. Interestingly, we found an approximately two-fold lower mean fluorescence intensity (MFI) for intracellular Igλ in Cre^{pos} iTIE/iTIE PCs, compared with Cre^{neg} iTIE/iTIE counterparts (Fig. 6 D). Hence, PCs expressing ΔV-κLCs synthesized low levels of Ig. Next, we evaluated whether the truncated Ig impaired the renewal or survival of PCs in Cre^{pos} and Cre^{neg} iTIE/iTIE mice injected with BrdU. Similar amounts of $BrdU^{neg}$ and $BrdU^{pos}$ B cells were retrieved for both strains (Fig. 6 E). In contrast, the frequency of $BrdU^{pos}$ (cycling) $B220^{neg}CD138^{pos}$ cells was significantly increased in Cre^{pos} iTIE mice compared with Cre^{neg} controls, indicating higher proportion of recently divided plasmablasts (PBs) upon production of ΔV-κLCs. Inversely, we found lower amounts of noncycling $BrdU^{neg}$ PCs in Cre^{pos} iTIE mice. Next, we sought to elucidate how the production of truncated Ig limited the lifespan of PCs. We analyzed the expression of ER stress markers, together with unfolded protein response (UPR) components in sorted PCs ($B220^{neg}CD138^{pos}$). In agreement with an exacerbated ER stress response upon production of ΔV-κLCs, *Chop*, *homocysteine-induced ER protein* (*Herp*), *X-box binding protein 1 spliced* (*Xbp1s*), and *BiP* mRNA levels were strongly increased in PCs isolated from Cre^{pos} iTIE mice (Fig. 6 F). Thus, the rise of ER stress as a result of the production of ΔV-κLCs is transiently tolerated in early differentiating PBs but clearly compromises their survival as noncycling long-lived PCs secreting high Ig amounts (Nutt et al., 2015).

Intrinsic toxicity of truncated Ig in plasma cells

ΔV-κLCs can induce multiple deleterious effects. On one hand, their presence could impede the normal assembly of IgH and IgL chains and relate to the classical quality control of BCR assembly (Melchers et al., 2000). On the other hand, the TIE checkpoint could involve an intrinsic toxicity of truncated Ig independent of BCR expression. To distinguish between these two hypotheses, we determined whether the elimination of PCs containing V^{PTC}-rearranged Igκ alleles also occurred in the absence of IgH chain expression. Igκ repertoires were thus compared between B cells ($B220^{pos}$) and PCs ($B220^{neg}/CD138^{pos}$) isolated from spleens of DH-LMP2A mice (Lechouane et al., 2013). In this model, the Epstein-Barr virus LMP2A protein mimics the BCR tonic signal and B lymphocytes develop without any IgH chain (Casola et al., 2004). As expected upon such a by-pass of BCR-driven positive selection, approximately two thirds of VκJκ5 junctions were out-of-frame in DH-LMP2A B cells, with an equivalent repartition of V^{PTC} and C^{PTC} subclasses (Table 2). Regarding nonproductive junctions, we found again that the V^{PTC} class was drastically decreased in PCs, compared with B cells (Table 2). In addition, we confirmed that the sole presence of ΔV-κLCs impaired PC differentiation by breeding iTIE mice on a DH-LMP2A background (Fig. 7 A). Thus, the elimination of PCs containing V^{PTC}-rearranged Igκ alleles occurred independent of IgH expression and BCR assembly. According to an exacerbated ER stress response and activation of the UPR, CHOP, HERP, BiP, *Xbp1s*, and IRE1α expression were strongly increased upon production of ΔV-κLCs (Fig. 7).

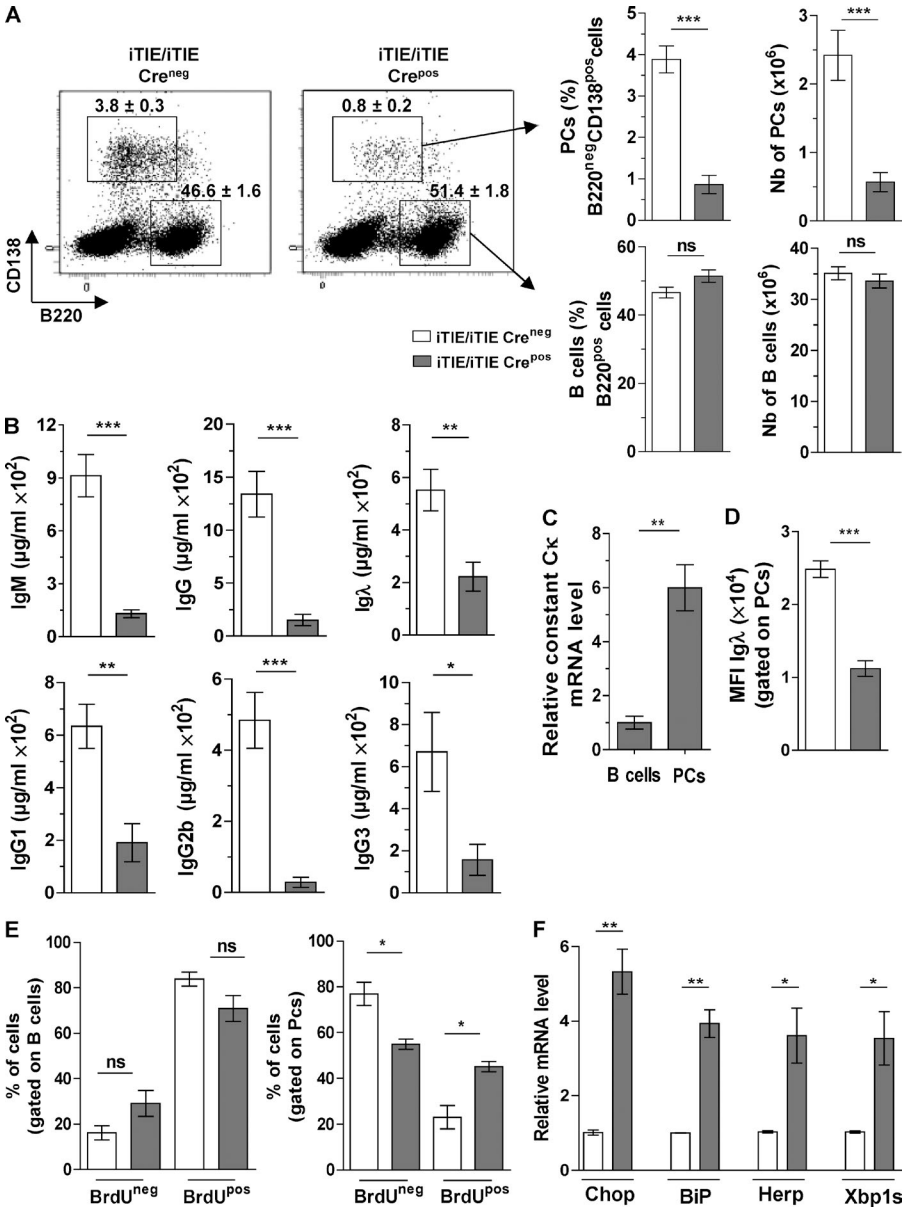

Figure 6. **PCs expressing ΔV-κLCs synthesize low amounts of Ig and preferentially accumulate as short-lived plasmablasts.** (A) Representative FACS analysis of spleen cells isolated from Cre^{pos} and Cre^{neg} homozygous iTIE/iTIE mice after staining with anti-B220 and anti-CD138 mAbs. The percentage and absolute numbers of B cells (B220^{pos}/CD138^{neg}) and PCs (B220^{neg}/CD138^{pos}) were determined on spleen cells (n = 6/group) isolated 7 d after IP injection of SRBCs. (B) ELISA assays were performed in sera from 8-wk-old Cre^{neg} (n = 9) and Cre^{pos} (n = 9) iTIE/iTIE mice to determine the amounts of Ig isotypes (IgM, Igλ, IgG1 IgG2b, IgG3, and total IgG). (C) Relative ΔV-κLC mRNA levels were determined in purified B cells (B220^{pos}/CD138^{neg}; n = 3) and PCs (B220^{neg}/CD138^{pos}; n = 3) sorted from spleens of iTIE/iTIE Cre^{pos} mice, 7 d after SRBC injection. RT-qPCR was performed using constant Cκ primers, after normalization to *Gapdh* transcripts. (D) Intracellular contents of Igλ were assessed by measuring the mean fluorescence intensity (MFI) in splenic Cre^{pos} (gray) and Cre^{neg} (empty) iTIE/iTIE B220^{neg}CD138^{pos} PCs (n = 6/group), 7 d after SRBC injection. (E) Cre^{pos} and Cre^{neg} iTIE/iTIE mice (n = 4/group) were injected with BrdU as described in experimental procedures. At day 10, the frequency of BrdU^{pos} (cycling) and BrdU^{neg} (noncycling) cells was analyzed in B cells (B220^{pos}CD138^{neg}; left) and PCs (B220^{neg}CD138^{pos}; right) isolated from bone marrow. (F) Relative mRNA levels of ER stress markers were assessed in purified PCs (B220^{neg}/CD138^{pos}) sorted from spleens of Cre^{pos} (gray; n = 3) and Cre^{neg} (empty; n = 3) iTIE/iTIE mice, 7 d after SRBC injection. Data are representative of at least two independent experiments. n = 3–9. Bars represent mean expression ± SEM. Unpaired two-tailed Student's test was performed to determine significance. *, P < 0.05; **, P < 0.01; ***, P < 0.001.

Table 2. **Analysis of productive and nonproductive VκJκ5 junctions in B and plasma cells from DH-LMP2A mice**

Cell type	Total	In-frame	V^{PTC}	C^{PTC}
	n	%	%	%
B cells	53	35.8	32.1	32.1
Plasma cells	55	67.3	5.4	27.3

B cells (B220^{pos}/CD138^{neg}) and PCs (B220^{neg}/CD138^{pos}) were isolated from spleens of DH-LMP2A mice and PCRs were performed on genomic DNA using Vκcons-for/Jκ5rev primers (Fig. 1 A). Productive and nonproductive VκJκ5 junctions were assigned as in-frame, V^{PTC}, and C^{PTC} junctions, as described in Table 1. Data are from two independent cell sorting experiments. n = total number of sequences.

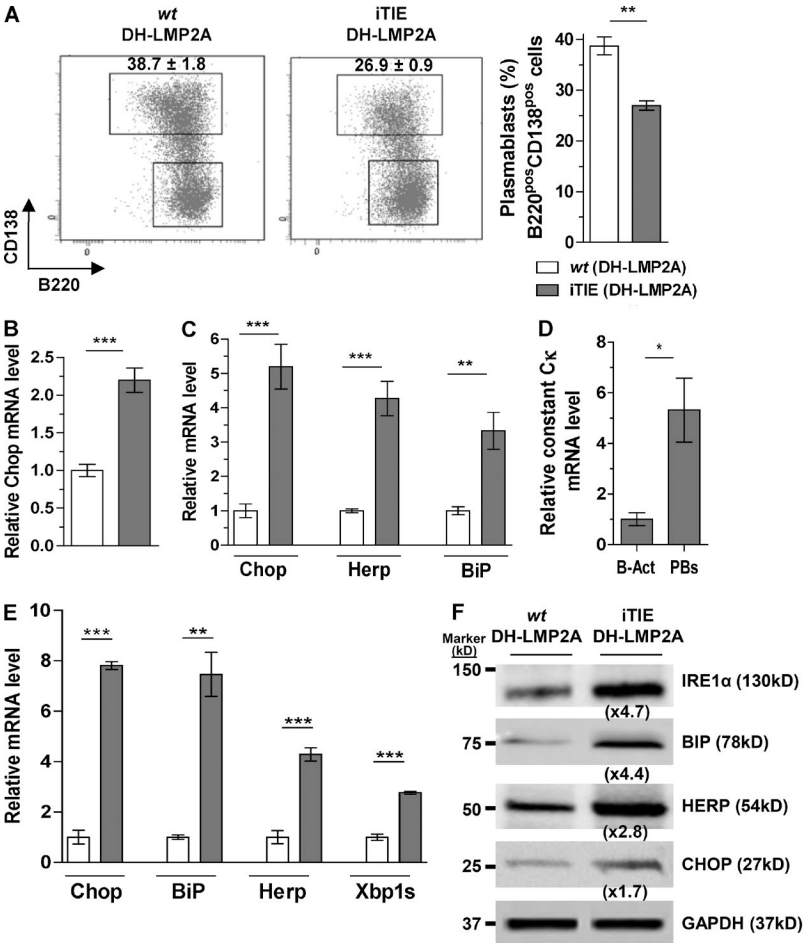

Figure 7. **Intrinsic toxicity of truncated Ig encoded by ΔV-κLC mRNAs.** Experiments were performed on the DH-LMP2A background lacking IgH expression to analyze intrinsic effects of ΔV-κLCs in terminally differentiated B lineage cells. (A) The frequency of ($B220^{pos}$/$CD138^{pos}$) plasmablasts (PBs) was determined in purified splenic B cells from iTIE/iTIE::DH-LMP2A (gray bars; $n = 4$) and *wt*/*wt*::DH-LMP2A (empty bars; $n = 4$) mice 4 d after LPS stimulation (1 µg/ml). The gates used are depicted in dot plots. (B and C) In those purified B cells, relative mRNA levels of ER stress markers were assessed at day 0 (B) or 4 d after LPS-stimulation (C). (D and E) The expression of ΔV-κLCs (D) and ER stress markers (E) was assessed in activated B cells (B-act: $B220^{pos}$/$CD138^{neg}$) and PBs ($B220^{pos}$/$CD138^{pos}$) sorted 4 d after LPS stimulation of B cells. (D) ΔV-κLC mRNA levels were assessed in the iTIE/iTIE::DH-LMP2A model by qPCR using Cκ primers, as described in Fig. 6 C. (E) *Chop*, *BiP*, *Herp*, and *Xbp1s* mRNA levels were assessed in purified PBs from iTIE/iTIE::DH-LMP2A mice (gray; $n = 3$), and compared with DH-LMP2A controls (empty; $n = 3$). Relative mRNA levels were determined after normalization to *Gapdh* transcripts. (F) To analyze CHOP, BIP, HERP, and IRE1α at the protein level, Western blots were performed in total LPS-stimulated B cells (day 4). A representative experiment is shown. Mean fold-change between iTIE/iTIE::DH-LMP2A ($n = 3$) and DH-LMP2A ($n = 3$) was calculated after normalization to GAPDH, using ImageJ software (National Institutes of Health). Data are representative of at least two independent experiments. $n = 3$–4. Bars represent mean expression ± SEM. Unpaired two-tailed Student's test was performed to determine significance. *, $P < 0.05$; **, $P < 0.01$; ***, $P < 0.001$.

Likewise, high ΔV-κLC mRNA levels were correlated with a strong expression of ER stress markers, in PBs sorted 4 d after LPS stimulation (Fig. 7, D and E). Altogether, these findings indicate that the TIE checkpoint is unrelated to a disturbed IgH/IgL assembly, but rather to a toxic ER stress provoked by the sole presence of ΔV-κLCs.

DISCUSSION

The allelic exclusion of Ig genes is stringently established before or during early B cell maturation and ensures the monospecificity of B lymphocytes through stepwise V(D)J recombination of Ig alleles. In cells harboring biallelic V(D)J rearrangements, the noise coming from transcription of nonproductive alleles has long been neglected because these transcripts are either degraded by NMD or do not encode functional Ig chains (Jäck et al., 1989; Li and Wilkinson, 1998; Delpy et al., 2004a; Chemin et al., 2010; Tinguely et al., 2012). However, we report here that alternative splicing of these passenger transcripts leads to the production of aberrant Ig chains that seriously impede PC differentiation. These findings identify a novel TIE checkpoint that eliminates ∼20–25% of terminally differentiated B lineage cells, i.e., those transcribing nonproductive Igκ alleles prone to exon skipping. Consistent with an Ag-independent checkpoint, ΔV-κLCs exert intrinsic toxic effects in PCs, likely mediated by ER stress–induced apoptosis. In addition, PCs expressing ΔV-κLCs synthesize low amounts of Ig and are mostly found among short-lived PBs. We propose that the TIE-checkpoint favors the selection of long-lived PCs with limited basal ER stress supporting high levels of Ig secretion.

Regarding nonproductively rearranged Igκ alleles, V^{PTC} and C^{PTC} junctions are highly similar and often exhibit a single nucleotide difference within the CDR3 sequences. Despite minor changes at the DNA level, we found that exon skipping was only enhanced for V^{PTC} class transcripts, with higher magnitude in PCs than in mature B cells. Although the molecular mechanisms underlying NAS are not completely understood, this response is triggered by two distinct pathways referred as class I and class II NAS (Maquat, 2002; Wang et al., 2002; Chang et al., 2007). Class I NAS occurs upon disruption of splicing motifs, such as exonic/intronic splicing enhancers/silencers, by either nonsense or missense mutations, whereas class II NAS is a reading frame–dependent process strictly induced by nonsense mutations (Chang et al., 2007). Thus, our data strongly suggest that a class II NAS response occurs for nonproductive Igκ transcripts that

further relies on PTC recognition within the skipped V exon, but not within the downstream Cκ exon. We also observed an approximately two-fold increase in ΔV-κLC mRNA levels in S194 plasma cells, compared with A20 B cells. In PCs, Ig genes are localized in transcription factories near the nuclear pore, and these specialized areas authorize cooperation of enhancers and facilitate Ig gene transcription (Park et al., 2014). In addition, a rise of exon skipping has been observed for highly transcribed genes, leading to the assumption that alternative splicing is closely correlated to the rate of RNA polymerase II elongation (Nogués et al., 2003; Shukla and Oberdoerffer, 2012). Altogether, we suggest that the boost of Ig gene transcription accompanying PC differentiation detrimentally promotes exon skipping during splicing of nonproductive Igκ premRNAs.

Biallelic Igκ rearrangements with a VJ^{+}/V^{PTC} configuration represent around 20–25% of mature B cells (Mostoslavsky et al., 2004) and hereby yield the population affected by the TIE checkpoint in terminally differentiated PCs. Sensitivity to prolonged ER stress likely explains the elimination of PCs producing ΔV-κLCs. Accordingly, ER stress markers and UPR components such as CHOP, BIP, HERP, and XBP1/IRE1α are up-regulated upon production of ΔV-κLCs in PCs. In addition, we found that *Chop* mRNA levels were already elevated in B cells expressing truncated Ig, suggesting that the early expression of this proapoptotic factor could influence the fate of differentiating PCs. Although a previous study showed that CHOP is dispensable for the development of LPS-induced plasmablasts (Masciarelli et al., 2010), our data are in agreement with a recent work highlighting its role in differentiating PCs (Gaudette et al., 2014) and also demonstrating that BCL-XL expression protects PCs from CHOP-associated apoptosis. The iTIE mouse model described herein should be useful to decipher the complex interplay between pro- and anti-apoptotic factors during PC differentiation.

With regard to PC dyscrasias, truncated Ig have been observed in some cases of myeloma (Cogné et al., 1988, 1992; Cogné and Guglielmi, 1993). However, it is a rare feature of primary PC dyscrasias and of malignant PC lines, suggesting that the TIE checkpoint also shapes the human Ig repertoire and that PCs producing aberrant Ig molecules are rarely rescued by oncogenic events (Decourt et al., 2004). Accordingly, we found that ΔV-κLCs were harmful for survival of normal PCs but exerted no obvious effect when expressed in tumor PCs in the absence of PI treatment. The survival of normal and malignant PCs is influenced by ER stress and the balance between load versus capacity of the proteasome (Cenci and Sitia, 2007). Being able to modulate ER stress and proteasome activity is of considerable interest for multiple myeloma (MM) patients (Meister et al., 2007) and new therapeutic strategies have emerged combining inhibitors of chaperones (Hsp90: Heat shock protein 90) or factors involved in unfolded protein response (IRE1α) with PI (Ishii et al., 2012; Mimura et al., 2012). Our findings are consistent with these combined approaches, increasing the amount of aberrant proteins while decreasing their proteasomal degradation, and suggest that splicing modulators or NMD inhibitors could also be useful tools to reinforce the production of truncated proteins including ΔV-κLCs.

Interestingly, the late TIE checkpoint stands as a quality control of individual and unassembled ΔV-κLCs and is not a result of a disturbance of BCR or secreted Ig assembly (which could then be viewed as a failed Ag response). Thus, the late occurrence of the TIE checkpoint, at the terminal differentiation stage, can be considered an intrinsic waste and weakness of the immune system. It allows uncensored B cells to accumulate as mature B cells carrying V^{PTC}-rearranged Igκ alleles, to potentially respond to Ag, and undergo affinity maturation in GCs, while being unable to yield long-lived PCs secreting high amounts of Ig (Nutt et al., 2015). The TIE checkpoint then cuts off the diversity of PCs arising from Ag-stimulated B cells for reasons unrelated to Ag recognition and affinity.

Whereas NMD basically protects cells from truncated protein synthesis, we show that activation of NAS herein exerts an opposite effect, finally ending with loss of ΔV-κLC–expressing PCs. This study thus shows that transcription and splicing of nonproductive Ig alleles, although often neglected or considered to be under control, are in fact often inappropriately handled by RNA surveillance pathways, allows production of truncated Ig and ends with a PC wastage.

MATERIALS AND METHODS

Gene targeting. Homologous recombination at the Igκ light chain locus was performed as described previously (Sirac et al., 2006). In brief, a 12.7-kb BamHI genomic fragment corresponding to the germline mouse JκCκ cluster was used to generate the iTIE targeting construct (Van Ness et al., 1982). A 2.2-kb BsmI–SacII fragment spanning all the Jκ segments was replaced with a cassette containing a V_H promoter (pV_H), a human leader exon ($L_{1\text{-}33}$), and a *lox*P-flanked neomycin-resistance gene driven by the Herpes simplex thymidine kinase promoter (*hsv*Tk-neoR). The *hsv*Tk-neoR cassette was inserted in opposite orientation to block the transcription and/or splicing of the $L_{1\text{-}33}$ exon (Fig. 4 A). Mouse embryonic stem cells (E14) were transfected with the linearized vector by electroporation and selected using 300 μg/ml Geneticin and 2 μM ganciclovir.

Mice. 2–3-mo-old mice were used in all experiments and maintained in our animal facilities, at 21–23°C with a 12-h light/dark cycle. Experiments were performed according to the guidelines of the ethics committee in Animal Experimentation of Limousin (registered by the National Committee under the number C2EA-33) and were approved as part of the protocol registered under the number CREEAL 6–07-2012. Heterozygous mutant mice (iTIE/+) were backcrossed to C57BL/6 (B6) for at least three generations, and then mated with Cre-expressing mice to induce deletion of the *hsv*Tk-neoR cassette. B6 CMV-Cre mice were obtained

from the Mouse Clinical Institute (Illkirch, France). B6 AID-Cre-EYFP mice, harboring a tamoxifen-inducible Cre recombinase enzyme controlled by the *Aicda* (activation-induced cytidine deaminase) promoter and a *lox*P-flanked EYFP (enhanced yellow fluorescent protein) reporter gene, have been described elsewhere (Dogan et al., 2009). B6 AID-Cre-EYFP mice were obtained from the Imagine Institute (Paris, France). In DH-LMP2A mice (with mixed B6/BALB/c backgrounds), the Epstein-Barr virus LMP2A protein drives B cell development and plasma cell differentiation, as previously described (Casola et al., 2004; Lechouane et al., 2013). DH-LMP2A mice were obtained from the Institute of Molecular Oncology Foundation (Milano, Italy).

Cell transfection. A20, S194, and Sp2/0 murine cell lines were cultured (10^6 cells/ml) in RPMI supplemented with 10% fetal calf serum (Invitrogen), sodium pyruvate, nonessential amino acids, β-mercaptoethanol, 100 U/ml penicillin, and 100 μg/ml streptomycin (Gibco). Cells (2×10^6) were stably transfected by electroporation according to the manufacturer's instructions (Amaxa). Transfections were performed using in-frame (F), V^{PTC}, and C^{PTC} linear plasmid constructs separately, or using equimolar ratios of F and nonproductive constructs as previously described (Chemin et al., 2010). Vκ Jκ5 junctions were built by artificially joining the $V\kappa_{1\text{-}135}$ and Jκ5 segments. To create a reading frameshift, 5 and 10 additional nt were introduced at the VκJκ junction in V^{PTC} and C^{PTC} constructs, respectively (Fig. 1 B). Cells (10^6 cells/ml) were treated or not with MG132 (1 μg/ml) for 5 or 8 h, as indicated, and control cells were treated with DMSO alone (dilution factor 1/1,000).

Flow cytometry and cell sorting. The frequency of apoptotic cells was determined after staining with Annexin V (BD) and propidium iodide using a LSRII Fortessa (BD). Data were analyzed with FACSDiva software (BD). Bone marrow B cell precursors and PCs were sorted on a FACSVantage (BD) after staining with anti–mouse B220 (RA3-6B2; BioLegend), anti–mouse Igκ (187–1; Beckman Coulter), anti–mouse Igλ (JC5-1; Beckman Coulter), and anti–mouse CD138 (281–2; BD) mAbs. The gates used for cell sorting are indicated in Fig. 3 A. GC B cells were isolated from Peyer's patches after staining with anti–mouse B220 and PNA (peanut agglutinin; Sigma-Aldrich) as previously described (Delpy et al., 2004b). In all experiments, purity of sorted cells was >90%. B cells were also isolated from spleens by negative selection using anti-CD43 microbeads (Miltenyi Biotec) and stimulated (0.5×10^6 cells/ml) with 1 μg/ml of LPS (LPS-EB Ultrapure; InvivoGen) for 4 d.

To determine the frequency of GC B cells and PCs, erythrocyte-depleted spleen cells were stained with anti-mouse GL7 (GL7; BD), anti-B220, and anti-CD138 mAbs, 7 d after intraperitoneal (IP) injection of sheep red blood cells (SRBCs; bioMérieux). When indicated, mice received additional subcutaneous bortezomib (Sillag) injections at day 5 and 6 (0.5 mg/kg). To induce nuclear translocation of Cre-recombinase, AID-Cre-EYFP mice were treated with Tamoxifen (1 μg/mouse, IP; Sigma-Aldrich) at day 2, 4, and 6 after SRBC immunization.

To analyze the renewal of B lineage cells in bone marrow, mice received i.p. BrdU (Sigma-Aldrich) injections (1 mg/mouse at day 0, then 0.5 mg every 48 h) for 10 d. Cells were then stained according to the BrdU Flow kit (BD) protocol. Cells were treated with DNase I before staining with anti-BrdU mAb. Intracellular Igλ staining was performed in bone marrow cells isolated from homozygous iTIE/iTIE mice using the Cytofix/Cytoperm kit (BD).

Western blot. For Western blot analysis, a 4–20% Mini-PROTEAN TGX polyacrylamide gel (Bio-Rad Laboratories) was used. Each sample was then denatured at 94°C for 3 min before being loaded. Gels were blotted onto TransBlot Turbo polyvinylidene fluoride membranes (Bio-Rad Laboratories), and blocked in PBST buffer (137 mM NaCl, 2.7 mM KCl, 10 mM Na_2HPO_4, 2 mM KH_2PO_4, and 0.1% Tween 20, pH 7.42) containing 5% nonfat dry milk. The signal was measured by chemoluminescence (ECL plus; GE Healthcare). Western blots were performed using rabbit anti-mouse HERP (Santa Cruz Biotechnology, Inc.), CHOP, BIP, IRE1α (Cell Signaling Technology), goat anti–mouse Igκ (Beckman Coulter), and using goat anti–mouse GAPDH (R&D Systems) Abs for normalization.

ELISA assays. Ig titers were determined in culture supernatants and mouse sera using unlabeled and alkaline phosphatase–conjugated goat anti–mouse Abs (IgM, IgG1, IgG3, IgG2b, Igκ, Igλ, and total IgG; Southern Biotech) as described (Pinaud et al., 2001; Sirac et al., 2006). Total Ig amounts were revealed by the addition of p-nitrophenyl phosphate (Sigma-Aldrich), and plates were read at 405 nm.

To analyze T cell–dependent humoral responses, mice received two IP injections with 10 μg hen egg OVA (Sigma-Aldrich) emulsified in 50% CFA (day 0) and IFA (day 14). For T cell–independent responses, mice received two IP injections (days 0 and 14) with 50 μg of 2,4, Dinitrophenyl-Amino-Ethyl-Carboxy-Methyl-Ficoll (DNP-Ficoll; Biosearch Technologies) emulsified in 50% IFA. Blood samples were collected (day 7 and 24) and antigen-specific antibody titers were determined in polycarbonate 96 multiwell plates (Maxisorp; Nunc) coated overnight at 4°C with OVA or albumin-DNP (Sigma-Aldrich) solution (10 μg/ml), in carbonate buffer.

PCR and RT-PCR. Genomic DNA and total RNA were prepared using standard proteinase K (Eurogentec) and Tri-reagent (Invitrogen) procedures, respectively. RT-PCR was performed on DNase I-treated (Invitrogen) RNA and was negative in the absence of reverse transcription, ruling out contamination by genomic DNA. Reverse transcription was performed using Superscript II (Invitrogen) on 1 to 5

μg of total RNA. Priming for reverse transcription was done with random hexamers.

Amplifications and capillary electrophoresis were performed as previously described (Chemin et al., 2010). Quantification of PCR products was also performed using an Agilent 2100 Bioanalyzer (Agilent Technologies) according to the Agilent High Sensitivity DNA kit instructions. Sequences of VκJκ5 junctions were analyzed after cloning of PCR products into pCR2.1-TOPO vector (Invitrogen), using V-QUEST software (IMGT, the international ImMunoGeneTics information system). Real-time PCR were performed on a ABI PRISM 7000 Sequence Detection System (Life Technologies). Transcripts were quantified according to the standard $2^{-\Delta\Delta Ct}$ method after normalization to *Gapdh*. Sequences of primers and probes are available upon request.

Statistical analysis. Results are expressed as mean ± SEM and overall differences between variables were evaluated by a two-tailed unpaired Student's *t* test using Prism GraphPad software. A χ^2 test was done to analyze the distribution of F, V^{PTC}, and $C^{PTC}V\kappa J\kappa$ junctions.

ACKNOWLEDGMENTS

We thank the staff of our animal facility, as well as C. Carrion and C. Ouk-Martin for technical assistance with microscopy and cell cytometry. We also thank K. Rajewsky (The Max Delbrück Center for Molecular Medicine, Berlin, Germany) and S. Casola (Institute of Molecular Oncology Foundation, Milano, Italy) for providing DH-LMP2A mice. AID-Cre-EYFP mice were kindly provided by CA Reynaud and JC Weill (Imagine Institute, Paris, France). We are grateful to J. Cook-Moreau (Centre National de la Recherche Scientifique UMR 7276, Limoges, France) for proofreading of the manuscript.

This work was supported by grants from Fondation ARC (#PGA120150202338 and SFI20121205821), Ligue Contre le Cancer (comité Haute-Vienne), Comité d'Organization de la Recherche sur le Cancer du Limousin (CORC), and Fondation pour la Recherche Médicale. N. Srour was funded by Conseil Régional du Limousin. A. Tinguely and G. Chemin were funded by French government fellowships.

The authors declare no competing financial interests.

Submitted: 17 July 2013
Accepted: 12 November 2015

REFERENCES

Allen, C.D.C., T. Okada, and J.G. Cyster. 2007. Germinal-center organization and cellular dynamics. *Immunity.* 27:190–202. http://dx.doi.org/10.1016/j.immuni.2007.07.009

Andrews, S.F., Q. Zhang, S. Lim, L. Li, J.-H. Lee, N.-Y. Zheng, M. Huang, W.M. Taylor, A.D. Farris, D. Ni, et al. 2013. Global analysis of B cell selection using an immunoglobulin light chain-mediated model of autoreactivity. *J. Exp. Med.* 210:125–142. http://dx.doi.org/10.1084/jem.20120525

Aoufouchi, S., J. Yélamos, and C. Milstein. 1996. Nonsense mutations inhibit RNA splicing in a cell-free system: recognition of mutant codon is independent of protein synthesis. *Cell.* 85:415–422. http://dx.doi.org/10.1016/S0092-8674(00)81119-8

Bertocci, B., A. De Smet, C. Berek, J.-C. Weill, and C.-A. Reynaud. 2003. Immunoglobulin κ light chain gene rearrangement is impaired in mice deficient for DNA polymerase mu. *Immunity.* 19:203–211. http://dx.doi.org/10.1016/S1074-7613(03)00203-6

Bühler, M., and O. Mühlemann. 2005. Alternative splicing induced by nonsense mutations in the immunoglobulin muVDJ exon is independent of truncation of the open reading frame. *RNA.* 11:139–146. http://dx.doi.org/10.1261/rna.718380515613538

Casola, S., K.L. Otipoby, M. Alimzhanov, S. Humme, N. Uyttersprot, J.L. Kutok, M.C. Carroll, and K. Rajewsky. 2004. B cell receptor signal strength determines B cell fate. *Nat. Immunol.* 5:317–327. http://dx.doi.org/10.1038/ni1036

Cenci, S., and R. Sitia. 2007. Managing and exploiting stress in the antibody factory. *FEBS Lett.* 581:3652–3657. http://dx.doi.org/10.1016/j.febslet.2007.04.031

Cenci, S., E. van Anken, and R. Sitia. 2011. Proteostenosis and plasma cell pathophysiology. *Curr. Opin. Cell Biol.* 23:216–222. http://dx.doi.org/10.1016/j.ceb.2010.11.004

Chang, Y.-F., W.-K. Chan, J.S. Imam, and M.F. Wilkinson. 2007. Alternatively spliced T-cell receptor transcripts are up-regulated in response to disruption of either splicing elements or reading frame. *J. Biol. Chem.* 282:29738–29747. http://dx.doi.org/10.1074/jbc.M704372200

Chemin, G., A. Tinguely, C. Sirac, F. Lechouane, S. Duchez, M. Cogné, and L. Delpy. 2010. Multiple RNA surveillance mechanisms cooperate to reduce the amount of nonfunctional Ig κ transcripts. *J. Immunol.* 184:5009–5017. http://dx.doi.org/10.4049/jimmunol.0902949

Chen, J., M. Trounstine, F.W. Alt, F. Young, C. Kurahara, J.F. Loring, and D. Huszar. 1993. Immunoglobulin gene rearrangement in B cell deficient mice generated by targeted deletion of the JH locus. *Int. Immunol.* 5:647–656. http://dx.doi.org/10.1093/intimm/5.6.647

Cogné, M., and P. Guglielmi. 1993. Exon skipping without splice site mutation accounting for abnormal immunoglobulin chains in nonsecretory human myeloma. *Eur. J. Immunol.* 23:1289–1293. http://dx.doi.org/10.1002/eji.1830230615

Cogné, M., A. Bakhshi, S.J. Korsmeyer, and P. Guglielmi. 1988. Gene mutations and alternate RNA splicing result in truncated Ig L chains in human gamma H chain disease. *J. Immunol.* 141:1738–1744.3137264

Cogné, M., C. Silvain, A.A. Khamlichi, and J.L. Preud'homme. 1992. Structurally abnormal immunoglobulins in human immunoproliferative disorders. *Blood.* 79:2181–2195.1571535

Daly, J., S. Licence, A. Nanou, G. Morgan, and I.-L. Mårtensson. 2007. Transcription of productive and nonproductive VDJ-recombined alleles after IgH allelic exclusion. *EMBO J.* 26:4273–4282. http://dx.doi.org/10.1038/sj.emboj.7601846

Decourt, C., H.R. Galea, C. Sirac, and M. Cogné. 2004. Immunologic basis for the rare occurrence of true nonsecretory plasma cell dyscrasias. *J. Leukoc. Biol.* 76:528–536. http://dx.doi.org/10.1189/jlb.0803382

Delpy, L., C. Sirac, E. Magnoux, S. Duchez, and M. Cogné. 2004a. RNA surveillance down-regulates expression of nonfunctional kappa alleles and detects premature termination within the last κ exon. *Proc. Natl. Acad. Sci. USA.* 101:7375–7380. http://dx.doi.org/10.1073/pnas.0305586101

Delpy, L., C. Sirac, C. Le Morvan, and M. Cogné. 2004b. Transcription-dependent somatic hypermutation occurs at similar levels on functional and nonfunctional rearranged IgH alleles. *J. Immunol.* 173:1842–1848. http://dx.doi.org/10.4049/jimmunol.173.3.1842

Dogan, I., B. Bertocci, V. Vilmont, F. Delbos, J. Mégret, S. Storck, C.-A. Reynaud, and J.-C. Weill. 2009. Multiple layers of B cell memory with different effector functions. *Nat. Immunol.* 10:1292–1299. http://dx.doi.org/10.1038/ni.1814

Eberle, A.B., K. Herrmann, H.-M. Jäck, and O. Mühlemann. 2009. Equal transcription rates of productively and nonproductively rearranged immunoglobulin mu heavy chain alleles in a pro-B cell line. *RNA.* 15:1021–1028. http://dx.doi.org/10.1261/rna.151640919363217

Ehlich, A., S. Schaal, H. Gu, D. Kitamura, W. Müller, and K. Rajewsky. 1993. Immunoglobulin heavy and light chain genes rearrange independently at

early stages of B cell development. *Cell*. 72:695–704. http://dx.doi.org/10.1016/0092-8674(93)90398-A

Frischmeyer-Guerrerio, P.A., R.A. Montgomery, D.S. Warren, S.K. Cooke, J. Lutz, C.J. Sonnenday, A.L. Guerrerio, and H.C. Dietz. 2011. Perturbation of thymocyte development in nonsense-mediated decay (NMD)-deficient mice. *Proc. Natl. Acad. Sci. USA*. 108:10638–10643. http://dx.doi.org/10.1073/pnas.1019352108

Gass, J.N., N.M. Gifford, and J.W. Brewer. 2002. Activation of an unfolded protein response during differentiation of antibody-secreting B cells. *J. Biol. Chem*. 277:49047–49054. http://dx.doi.org/10.1074/jbc.M205011200

Gaudette, B.T., N.N. Iwakoshi, and L.H. Boise. 2014. Bcl-xL protein protects from C/EBP homologous protein (CHOP)-dependent apoptosis during plasma cell differentiation. *J. Biol. Chem*. 289:23629–23640. http://dx.doi.org/10.1074/jbc.M114.569376

Holwerda, S.J.B., H.J.G. van de Werken, C. Ribeiro de Almeida, I.M. Bergen, M.J.W. de Bruijn, M.J.A.M. Verstegen, M. Simonis, E. Splinter, P.J. Wijchers, R.W. Hendriks, and W. de Laat. 2013. Allelic exclusion of the immunoglobulin heavy chain locus is independent of its nuclear localization in mature B cells. *Nucleic Acids Res.* 41:6905–6916. http://dx.doi.org/10.1093/nar/gkt491

Ishii, T., T. Seike, T. Nakashima, S. Juliger, L. Maharaj, S. Soga, S. Akinaga, J. Cavenagh, S. Joel, and Y. Shiotsu. 2012. Anti-tumor activity against multiple myeloma by combination of KW-2478, an Hsp90 inhibitor, with bortezomib. *Blood Cancer J.* 2:e68. http://dx.doi.org/10.1038/bcj.2012.13

Jäck, H.M., J. Berg, and M. Wabl. 1989. Translation affects immunoglobulin mRNA stability. *Eur. J. Immunol*. 19:843–847. http://dx.doi.org/10.1002/eji.1830190510

Jung, D., C. Giallourakis, R. Mostoslavsky, and F.W. Alt. 2006. Mechanism and control of V(D)J recombination at the immunoglobulin heavy chain locus. *Annu. Rev. Immunol*. 24:541–570. http://dx.doi.org/10.1146/annurev.immunol.23.021704.115830

Lechouane, F., A. Bonaud, L. Delpy, S. Casola, Z. Oruc, G. Chemin, M. Cogné, and C. Sirac. 2013. B cell receptor signal strength influences terminal differentiation. *Eur. J. Immunol*. 43:619–628. http://dx.doi.org/10.1002/eji.201242912

Lejeune, F., and L.E. Maquat. 2005. Mechanistic links between nonsense-mediated mRNA decay and pre-mRNA splicing in mammalian cells. *Curr. Opin. Cell Biol*. 17:309–315. http://dx.doi.org/10.1016/j.ceb.2005.03.002

Li, S., and M.F. Wilkinson. 1998. Nonsense surveillance in lymphocytes? *Immunity*. 8:135–141. http://dx.doi.org/10.1016/S1074-7613(00)80466-5

Lutz, J., M.R. Heideman, E. Roth, P. van den Berk, W. Müller, C. Raman, M. Wabl, H. Jacobs, and H.-M. Jäck. 2011. Pro–B cells sense productive immunoglobulin heavy chain rearrangement irrespective of polypeptide production. *Proc. Natl. Acad. Sci. USA*. 108:10644–10649. http://dx.doi.org/10.1073/pnas.1019224108

Manis, J.P., M. Tian, and F.W. Alt. 2002. Mechanism and control of class-switch recombination. *Trends Immunol*. 23:31–39. http://dx.doi.org/10.1016/S1471-4906(01)02111-1

Maquat, L.E. 2002. NASty effects on fibrillin pre-mRNA splicing: another case of ESE does it, but proposals for translation-dependent splice site choice live on. *Genes Dev.* 16:1743–1753. http://dx.doi.org/10.1101/gad.1014502

Masciarelli, S., A.M. Fra, N. Pengo, M. Bertolotti, S. Cenci, C. Fagioli, D. Ron, L.M. Hendershot, and R. Sitia. 2010. CHOP-independent apoptosis and pathway-selective induction of the UPR in developing plasma cells. *Mol. Immunol*. 47:1356–1365. http://dx.doi.org/10.1016/j.molimm.2009.12.003

Meister, S., U. Schubert, K. Neubert, K. Herrmann, R. Burger, M. Gramatzki, S. Hahn, S. Schreiber, S. Wilhelm, M. Herrmann, et al. 2007. Extensive immunoglobulin production sensitizes myeloma cells for proteasome inhibition. *Cancer Res.* 67:1783–1792. http://dx.doi.org/10.1158/0008-5472.CAN-06-2258

Melchers, F., E. ten Boekel, T. Seidl, X.C. Kong, T. Yamagami, K. Onishi, T. Shimizu, A.G. Rolink, and J. Andersson. 2000. Repertoire selection by pre-B-cell receptors and B-cell receptors, and genetic control of B-cell development from immature to mature B cells. *Immunol. Rev.* 175:33–46. http://dx.doi.org/10.1111/j.1600-065X.2000.imr017510.x

Mimura, N., M. Fulciniti, G. Gorgun, Y.-T. Tai, D. Cirstea, L. Santo, Y. Hu, C. Fabre, J. Minami, H. Ohguchi, et al. 2012. Blockade of XBP1 splicing by inhibition of IRE1α is a promising therapeutic option in multiple myeloma. *Blood*. 119:5772–5781. http://dx.doi.org/10.1182/blood-2011-07-366633

Mostoslavsky, R., F.W. Alt, and K. Rajewsky. 2004. The lingering enigma of the allelic exclusion mechanism. *Cell*. 118:539–544. http://dx.doi.org/10.1016/j.cell.2004.08.023

Mühlemann, O., C.S. Mock-Casagrande, J. Wang, S. Li, N. Custódio, M. Carmo-Fonseca, M.F. Wilkinson, and M.J. Moore. 2001. Precursor RNAs harboring nonsense codons accumulate near the site of transcription. *Mol. Cell*. 8:33–43. http://dx.doi.org/10.1016/S1097-2765(01)00288-X

Nogués, G., S. Kadener, P. Cramer, M. de la Mata, J.P. Fededa, M. Blaustein, A. Srebrow, and A.R. Kornblihtt. 2003. Control of alternative pre-mRNA splicing by RNA Pol II elongation: faster is not always better. *IUBMB Life*. 55:235–241. http://dx.doi.org/10.1080/1521654031000119830

Novobrantseva, T.I., V.M. Martin, R. Pelanda, W. Müller, K. Rajewsky, and A. Ehlich. 1999. Rearrangement and expression of immunoglobulin light chain genes can precede heavy chain expression during normal B cell development in mice. *J. Exp. Med*. 189:75–88. http://dx.doi.org/10.1084/jem.189.1.75

Nutt, S.L., P.D. Hodgkin, D.M. Tarlinton, and L.M. Corcoran. 2015. The generation of antibody-secreting plasma cells. *Nat. Rev. Immunol*. 15:160–171. http://dx.doi.org/10.1038/nri3795

Obeng, E.A., L.M. Carlson, D.M. Gutman, W.J.J. Harrington Jr., K.P. Lee, and L.H. Boise. 2006. Proteasome inhibitors induce a terminal unfolded protein response in multiple myeloma cells. *Blood*. 107:4907–4916. http://dx.doi.org/10.1182/blood-2005-08-3531

Park, S.-K., Y. Xiang, X. Feng, and W.T. Garrard. 2014. Pronounced cohabitation of active immunoglobulin genes from three different chromosomes in transcription factories during maximal antibody synthesis. *Genes Dev.* 28:1159–1164. http://dx.doi.org/10.1101/gad.237479.114

Pavri, R., and M.C. Nussenzweig. 2011. AID targeting in antibody diversity. *Adv. Immunol*. 110:1–26. http://dx.doi.org/10.1016/B978-0-12-387663-8.00005-3

Péron, S., B. Laffleur, N. Denis-Lagache, J. Cook-Moreau, A. Tinguely, L. Delpy, Y. Denizot, E. Pinaud, and M. Cogné. 2012. AID-driven deletion causes immunoglobulin heavy chain locus suicide recombination in B cells. *Science*. 336:931–934. http://dx.doi.org/10.1126/science.1218692

Pinaud, E., A.A. Khamlichi, C. Le Morvan, M. Drouet, V. Nalesso, M. Le Bert, and M. Cogné. 2001. Localization of the 3′ IgH locus elements that effect long-distance regulation of class switch recombination. *Immunity*. 15:187–199. http://dx.doi.org/10.1016/S1074-7613(01)00181-9

Rajewsky, K. 1996. Clonal selection and learning in the antibody system. *Nature*. 381:751–758. http://dx.doi.org/10.1038/381751a0

Ron, D., and P. Walter. 2007. Signal integration in the endoplasmic reticulum unfolded protein response. *Nat. Rev. Mol. Cell Biol*. 8:519–529. http://dx.doi.org/10.1038/nrm2199

Santos, P., F. Arumemi, K.S. Park, L. Borghesi, and C. Milcarek. 2011. Transcriptional and epigenetic regulation of B cell development. *Immunol. Res.* 50:105–112. http://dx.doi.org/10.1007/s12026-011-8225-y

Shukla, S., and S. Oberdoerffer. 2012. Co-transcriptional regulation of alternative pre-mRNA splicing. *Biochim. Biophys. Acta.* 1819:673–683. http://dx.doi.org/10.1016/j.bbagrm.2012.01.014

Singh, N., Y. Bergman, H. Cedar, and A. Chess. 2003. Biallelic germline transcription at the κ immunoglobulin locus. *J. Exp. Med.* 197:743–750. http://dx.doi.org/10.1084/jem.20021392

Sirac, C., F. Bridoux, C. Carrion, O. Devuyst, B. Fernandez, J.-M. Goujon, C. El Hamel, J.-C. Aldigier, G. Touchard, and M. Cogné. 2006. Role of the monoclonal κ chain V domain and reversibility of renal damage in a transgenic model of acquired Fanconi syndrome. *Blood.* 108:536–543. http://dx.doi.org/10.1182/blood-2005-11-4419

Tinguely, A., G. Chemin, S. Péron, C. Sirac, S. Reynaud, M. Cogné, and L. Delpy. 2012. Cross talk between immunoglobulin heavy-chain transcription and RNA surveillance during B cell development. *Mol. Cell. Biol.* 32:107–117. http://dx.doi.org/10.1128/MCB.06138-11

Todd, D.J., L.J. McHeyzer-Williams, C. Kowal, A.-H. Lee, B.T. Volpe, B. Diamond, M.G. McHeyzer-Williams, and L.H. Glimcher. 2009. XBP1 governs late events in plasma cell differentiation and is not required for antigen-specific memory B cell development. *J. Exp. Med.* 206:2151–2159. http://dx.doi.org/10.1084/jem.20090738

Valentine, C.R. 1998. The association of nonsense codons with exon skipping. *Mutat. Res.* 411:87–117. http://dx.doi.org/10.1016/S1383-5742(98)00010-6

Van Ness, B.G., C. Coleclough, R.P. Perry, and M. Weigert. 1982. DNA between variable and joining gene segments of immunoglobulin κ light chain is frequently retained in cells that rearrange the kappa locus. *Proc. Natl. Acad. Sci. USA.* 79:262–266. http://dx.doi.org/10.1073/pnas.79.2.262

Victora, G.D., and M.C. Nussenzweig. 2012. Germinal centers. *Annu. Rev. Immunol.* 30:429–457. http://dx.doi.org/10.1146/annurev-immunol-020711-075032

Wang, J., J.I. Hamilton, M.S. Carter, S. Li, and M.F. Wilkinson. 2002. Alternatively spliced TCR mRNA induced by disruption of reading frame. *Science.* 297:108–110. http://dx.doi.org/10.1126/science.1069757

Weischenfeldt, J., I. Damgaard, D. Bryder, K. Theilgaard-Mönch, L.A. Thoren, F.C. Nielsen, S.E.W. Jacobsen, C. Nerlov, and B.T. Porse. 2008. NMD is essential for hematopoietic stem and progenitor cells and for eliminating by-products of programmed DNA rearrangements. *Genes Dev.* 22:1381–1396. http://dx.doi.org/10.1101/gad.468808